Materials Research Bulletin 49 (2014) 521–524

Contents lists available at ScienceDirect

Materials Research Bulletin

journal homepage: www.elsevier.com/locate/matresbu

Preparation of nickel nanoparticle/graphene composites for non-enzymatic electrochemical glucose biosensor applications

Bo Wang, Songmei Li *, Jianhua Liu, Mei Yu

School of Materials Science and Engineering, Beihang University, Beijing 100191, PR China

ARTICLE INFO

Article history:
Received 2 February 2013
Received in revised form 14 August 2013
Accepted 29 August 2013
Available online 7 September 2013

Keywords:
A. Composites
B. Chemical synthesis
C. Electrochemical measurements
C. Electron microscopy

ABSTRACT

A novel non-enzymatic electrochemical sensor device was fabricated for glucose detection based on nickel nanoparticles/graphene nanosheets (NiNPs/GNs) composites, which were synthesized through in situ chemical reduction procedure. The NiNPs/GNs composites modified electrode exhibited high electrocatalytic activity and good response toward the oxidation of glucose in alkaline solution, attributing to the synergistic effect of GNs and NiNPs. At detection potential of +0.5 V, the biosensor exhibited high sensitivity of 865 $\mu A\,mM^{-1}\,cm^{-2}$ for glucose with a wide linear range from 5 μM to 550 μM as well as a low detection limit of 1.85 μM (at a signal-to-noise ratio(S/N) of 3). The good analytical performance, low cost and simple fabrication procedure make this novel electrode material promising for the development of effective non-enzymatic glucose sensor.

1. Introduction

Graphene is a new class of two-dimensional nanomaterial consisting of a single layer of sp^2 network of carbon atoms [1]. Due to a host of intriguing properties such as high surface area, good biocompatibility, excellent electrical conductivity and ease of functionalization and production [2–4], GNs provides an ideal platform to prepare functional nanomaterials for biosensors. Recently, GNs have been successfully combined with metal nanoparticles and applied to the fabrication of non-enzymatic glucose sensors [5]. The combination of metal NPs and GNs not only prohibits the aggregation and oxidation of the metal NPs but also improve the performances of electrodes.

Ni-based nanomaterials exhibited remarkably catalytic oxidation activity over glucose as result of the catalytic effect originating from the formation of the redox couple of Ni(II)/Ni(III) on the electrode surface in alkaline medium[6,7]. Considering the attractive properties of GNs, it is quite expected that GNs could provide an excellent support of the NiNPs for efficient electron transfer toward the oxidation of glucose. In addition, different morphological Ni nanostructures have been successfully synthesized via different methods in past decades. The high surface area-to-volume ratios of urchin-like nanostructures could increase the voltammetric signals for electroactive species that diffused from the bulk solution [8,9].

In this paper, a facile in situ synthetic route was used to prepare urchin-like NiNPs/GNs composites, and then the as-fabricated NiNPs/GNs modified glassy carbon electrode (GCE) was reported with high electrocatalytic activity toward the oxidation of glucose. Meanwhile, the interference was also investigated.

2. Experimental

Graphite oxide (GO) was synthesized from natural graphite by a modified Hummers method [10]. NiNPs/GNs composites were prepared by in situ reducing reaction of GO and Ni-hydrazine complex using hydrazine hydrate. 100 mg of GO was dispersed into 50 mL of deionized (DI) water with ultrasonication for 1 h to form a stable GO suspension. 20 mL of an aqueous $NiCl_2{\cdot}6H_2O$ solution (0.07 M) and 40 mL of $N_2H_4{\cdot}H_2O$ were mixed with vigorous stirring to give a Ni–hydrazine complex suspension. The Ni–hydrazine complex suspension was added into GO solution and stirred for another 30 min. Subsequently, 20 mL of hydrazine hydrate and 40 mg of NaOH were added into the mixed solution, followed by ultrasonication for 15 min. After that, the above mixture was transferred into a 250 mL round-bottomed flask and refluxed at 100 °C for 5 h. After cooled to room temperature naturally, the as-synthesized solid products were collected by vacuum filtration, washed with DI water and ethanol for three times to remove the excess chemicals. The final product was then dried in a vacuum oven at 60 °C for 24 h to obtain the dried NiNPs/GNs nanocomposites.

The morphologies and microstructure of the samples were investigated by powder X-ray diffraction system (XRD, Rigaku

* Corresponding author. Tel.: +86 10 82317103; fax: +86 10 82317103.
E-mail address: songmei_li@buaa.edu.cn (S. Li).

0025-5408/$ – see front matter © 2013 Elsevier Ltd. All rights reserved.
http://dx.doi.org/10.1016/j.materresbull.2013.08.066

D/max 2200PC), scanning electron microscope (SEM, Hitachi S-4800, Japan), transition electron microscope (TEM, JEOL JEM-2100, Japan). Raman spectra were recorded using Jobin Yvon Labram HR800 (excitation wavelength: 632.8 nm). Fourier transform infrared (FT-IR) spectra were obtained on a Nicolet Nexus 470 spectrophotometer with KBr pellets in the 4000–400 cm^{-1} region. All electrochemical experiments including cyclic voltammetry (CV) and amperometry were carried out using a CHI 660A electrochemical work Station. Electrochemical measurements were performed in 0.1 M NaOH supporting electrolyte at room temperature using a three-electrode system consisting of a KCl saturated calomel electrode (SCE) as the reference electrode, a platinum sheet as the counter electrode, and the NiNPs/GNs modified GCEs as the working electrode. The NiNPs/GNs modified GCE was fabricated by dripping 10 μL of the NiNPs/GNs dispersion onto the GCE surface and dried 12 h in air. The NiNPs/GNs dispersion was prepared by dispersed 10 mg GNs–NiNPs composites in 10 mL of deionized water containing 40 μL of Nafion solution (5 wt.%) with sonication for 10 min.

3. Results and discussion

Fig. 1 shows the XRD patterns of the as-prepared GO (a) and NiNPs/GNs composites (b). As displayed in curve a, the most intensive peak of GO at around $2\theta = 11.6^\circ$ corresponds to the (0 0 1) reflection but in curve b the peak at the same position disappears, meanwhile, new diffraction peaks assigned to graphene at 26.7° and 54.64° (corresponding to the indices of (0 0 2) and (1 0 0)) can be observed in curve b, indicating that graphene oxide has been reduced to graphene accompanied with the removal of oxygen groups when forming NiNPs/GNs composites [11]. The three diffraction peaks in curve b centered at $2\theta = 44.30^\circ$, 51.78°, and 76.29° are corresponding to the (1 1 1), (2 0 0), and (2 2 0) crystal planes of the face-centered cubic (fcc) Ni (JCPDS, file No. 04-0850), respectively. The XRD results indicated that the GO nanosheets were reduced to GNs during the in situ chemical reduction process, while the NiNPs were also formed in this process.

The morphology and structure of the as-prepared urchin-like NiNPs/GNs composites were characterized by SEM and TEM as shown in Fig. 2. It is clearly seen in Fig. 2(A and B) that the urchin-like NiNPs were uniformly distributed and embedded throughout the graphene matrix and an interconnected hybrid network has formed. The diameter of NiNPs was estimated to be 200 nm. The high-resolution SEM and TEM images shown in Fig. 2(B and C) exhibits that urchin-like morphology consisted of a spherical core attached with various spear-like branches. A high-resolution TEM image focusing on a spear-like branches was shown in Fig. 2(D). Crystal fringes are clearly displayed, and the fringe spacing of this nanoparticle is determined to be 0.2 and 0.18 nm, corresponding to the spacing of (1 1 1) and (2 0 0) planes of fcc Ni.

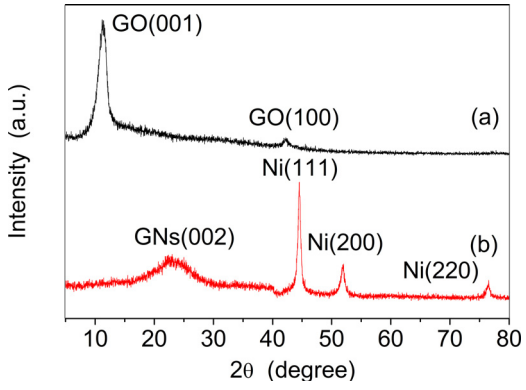

Fig. 1. XRD patterns of the as-prepared GO (a) and NiNPs/GNs composites (b).

Fig. 3 shows the Raman spectra of the as-prepared GO and NiNPs/GNs composites. The Raman spectrum of graphene is usually characterized by two main features, the G mode arising from the first-order scattering of the E_{2g} phonon of sp^2 C atoms and the D mode arising from a breathing mode of κ-point photons of A_{1g} symmetry [12]. It can be clearly seen from Fig. 3 that GO exhibits a D band at 1355 cm^{-1} and a G band at 1590 cm^{-1}, while the corresponding bands of NiNPs/GNs composites are 1350 and 1580 cm^{-1}, respectively. It is a general feature for the reduction of the GO that the G band shifts to a lower number. As shown in Fig. 3, the G band of NiNPs/GNs shifts to 1580 cm^{-1} compared to 1590 cm^{-1} of GO, indicating the restoration of the conjugated π systems[13]. Another Raman spectral feature for the reduction of GO is that the peak intensity ratio (I_D/I_G) between D band and G band, After the reduction by hydrazine hydrate, the I_D/I_G increases from 0.96 to 1.34. This result can be ascribed to the restoration of numerous graphitic domains from amorphous regions of GO, which gives rise to stronger D band signal [14].

The FT-IR spectra of GO and NiNPs/GNs composites are shown in Fig. 4. The characteristic IR features of GO indicate the presence of the oxygen-containing functional groups on the surface of GO. As illustrated in Fig. 4, the characteristic bands of GO are observed at 3433, 1726, and 1042 cm^{-1}, which are attributed to the stretching vibrations of O–H, C=O, and C–O–C, respectively. The peaks at 1630 and 1173 cm^{-1} correspond to the vibration of carboxyl groups [15]. After the reduction by hydrazine hydrate, these peaks become weak or disappear. The results imply that the number of epoxy, hydroxyl, carbonyl, and carboxyl groups in NiNPs/GNs composites substantially decreased after chemical reduction [16].

The electrocatalytic activities of the GNs, NiNPs and NiNPs/GNs modified GCE were investigated using cyclic voltammetry (CV) in 0.1 M NaOH solution in the absence and presence of 1 mM glucose at a scan rate of 50 mV s^{-1}. As shown in Fig. 5(A), in the absence of glucose (curve c), one pair of well-defined redox peaks for the NiNPs/GNs modified GCE can be observed. Upon the addition of glucose, there is no reaction peak current observed for the GNs (curve a) modified GCE at the electrochemical window. In the cyclic voltammograms (curve b and d) at the NiNPs and NiNPs/GNs modified GCE, a pair of asymmetric redox peaks can be observed. Of them, the peak currents obtained at the NiNPs/GNs modified electrode were significantly increased, indicating that the NiNPs/GNs composites exhibit excellent electrocatalytic activity toward the oxidation of glucose. As indicated in the literatures [12,13], the response mechanism of the NiNPs/GNs modified SCE to electrochemical oxidation of glucose can be simply expressed as:

$$Ni(OH)_2 + H^- \rightarrow NiO(OH) + H_2O + e^- \quad (1)$$

$$NiO(OH) + \text{Glucose} \rightarrow Ni(OH)_2 + \text{Glucolactone} \quad (2)$$

Fig. 5(B) depicts the CVs of the NiNPs/GNs modified GCE in 0.1 M NaOH solution containing 1 mM glucose at different scan rates. As shown in Fig. 5(B), the anodic peak current due to oxidation of glucose increased with increasing scan rates while the anodic peak potential shifted to more positive values. It may be due to the diffusion limitation of glucose at the electrode surface. The plot of the oxidation and reduction peak currents against the square root of scan rates (inset in Fig. 5(B)) shows an excellent linear direct relationship, which suggests that the electrocatalytic process was controlled by glucose diffusion to the modified electrode/solution interface.

The amperometric responses of the as-prepared NiNPs/GNs modified GCE nonenzymatic glucose sensing with the successive addition of glucose at 50 s intervals in 0.1 M NaOH at an applied